This paper describes objective technical results and analysis. Any subjective views or opinions that might be expressed in the paper do not necessarily represent the views of the U.S. Department of Energy or the United States Government.

SAND2019-10193C

A Method for Correcting Frequency and RoCoF Estimates of Power System Signals with Phase Steps

Felipe Wilches-Bernal
Sandia National Laboratories
Albuquerque, NM
fwilche@sandia.gov

Josh Wold
Montana Technological University
Butte, MT
jwold@mtech.edu

Ricky Concepcion
Sandia National Laboratories
Albuquerque, NM
rconcep@sandia.gov

Jamie Budai
Georgia Institute of Technology
Atlanta, GA
jbudai6@gatech.edu

***Abstract*—This paper analyzes how two Kalman Filter (KF) based frequency estimation algorithms react to phase steps. It is demonstrated that phase steps are interpreted as sharp changes in frequency. The paper studies whether the location of the phase step, within the sinusoidal waveform, has any effect on the frequency estimate. Because phase steps are not the product of a permanent change in the underlying frequency, the paper proposes an algorithm to correct frequency estimates deemed erroneous. The algorithm makes use of the residual of the KF to determine when an estimate is incorrect and to trigger a corrective action in which the frequency estimate is replaced by an average of the previous values that were considered accurate. Using synthesized and simulated data with distortions the paper shows the effectiveness of the correction algorithm in fixing frequency estimates.**

***Index Terms*—Kalman Filter, Frequency Estimation, Point on Wave, Phase Jumps**

I. Introduction

Frequency and rate of change of frequency (RoCoF) in a power system indicate how well the system is behaving. A stable power system is expected to have very few frequency fluctuations and RoCoF values near zero most of the time. Accurate measurement of frequency and RoCoF is crucial for power system stability and control. Frequency measurements are used to drive droop controllers and for under frequency load shedding (UFLS). The work in [1] identified three use cases for RoCoF: (i) loss of mains protection, (ii) UFLS, and (iii) synthetic inertia controllers.

In the power system community point on wave (POW) data refers to the sampled data of power system signals without undergoing any major processing. These data are the sinusoidal waveforms sampled at rates on the order of kHz which are much higher than the traditional SCADA and PMU data. Even though the problem of estimating frequency from POW data has been studied considerably in the past [2], there is a renewed interest due to the particular challenges facing the power industry today such as the increase in converter interfaced generation [1], [3]. For example, the 1200 MW interruption of solar power event experienced in California in August of 2016 was partially attributed to faulty frequency estimates [4].

Frequency and RoCoF estimation of heavily distorted waveforms is a challenge. One of the distortions that has received more attention recently is phase steps (or jumps) [1], [3], [5], [6]. The work in [3], [5] shows that phase jumps in the POW data can to lead to *erroneous* frequency and RoCoF estimates from measurement equipment such as PMUs.

This paper analyzes the effect that phase steps have on the frequency estimation of two previously proposed frequency estimation algorithms [7]–[9]. The algorithms under consideration are based on the Kalman Filter (KF) which is a tool to optimally estimate the parameters of interest of a signal. Specifically, one of the methods is based on the Extended Kalman Filter (EKF) while the other uses the Unscented Kalman Filter (UKF) to address the nonlinearities of the process under consideration. The paper considers two type of phase steps, one of them coming from synthesized sinusoidal waveforms and the other from simulated data of power system line faults. The paper shows that phase steps, in which the *underlying* frequency is not modified, strongly affect the frequency estimate of the evaluated algorithms. Specifically, phase steps cause the estimated frequency to diverge steeply from the nominal. The paper also studies what effect the location of the phase step within the sinusoidal waveform has on the frequency estimate. The results show that a phase step occurring when the sinusoidal waveform is reaching its maximum (within a period) cause more disruption to the estimate than when it occurs in other places. Additionally, this paper proposes an algorithm to correct frequency estimates when they are deemed inaccurate. In the proposed algorithm the estimates are determined as inaccurate when the residual of the KF surpasses a user-specified threshold. The proposed

Sandia National Laboratories is a multimission laboratory managed and operated by National Technology and Engineering Solutions of Sandia, LLC., a wholly owned subsidiary of Honeywell International, Inc., for the U.S. Department of Energy's National Nuclear Security Administration under contract DE-NA0003525.

This research was supported by the U.S. Department of Energy Advanced Grid Modeling (AGM) program.

978-1-7281-0407-2/19/$31.00 © 2019 IEEE

algorithm is tested with both the synthesized and the simulated data and it is shown that it is able to correct all the frequency estimates. In this work the RoCoF estimate is obtained directly as the derivative of the frequency estimate so any correction to the frequency estimate is reflected in the RoCoF estimate. The corrected frequency and RoCoF signal produced by the proposed algorithm are clearly preferred for any control action.

The rest of the paper is organized as follows. Section II presents the framework for process estimation using both the EKF and UKF methods. Section III shows how frequency and RoCoF are estimated based on the KF methods from the previous section and introduces the algorithm for frequency correction. Section IV shows the result of frequency and RoCoF estimation and correction for the two sets of data considered. Finally, Section V presents the conclusions and future work.

II. Kalman Filter for Frequency Estimation

A. Signal Model

In a stable power system an adequate model to represent single phase voltage or current signals is

$$z(t) = A(t)\cos(\omega t + \phi(t)) \tag{1}$$

where $\omega = 2\pi f_0$, and f_0 is the nominal grid frequency with a value of 60 Hz in North America. Sampling the signal in (1) with a period of T_s yields

$$z_k = A\cos(\omega t_k + \phi(t_k)) \quad k = 1, \ldots, N \tag{2}$$

with $t_k = kT_s$. Note that in (2) the amplitude of the signal A was assumed constant, a valid assumption for most power system signals over short time scales and in relatively stable conditions. Using Euler's equation, relationship (2) can be rewritten as

$$z_k = \frac{A}{2}\left(e^{j(\omega t_k + \phi(t_k))} + e^{-j(\omega t_k + \phi(t_k))}\right) \tag{3}$$

Defining four states of complex sinusoidal signals as follows

$$x_{1,k} = e^{j\omega T_s} \qquad x_{3,k} = e^{-j\omega T_s} \tag{4}$$

$$x_{2,k} = Ae^{j(\omega k T_s + \phi(t_k))} \qquad x_{4,k} = Ae^{-j(\omega k T_s + \phi(t_k))} \tag{5}$$

will yield the following state space representation

$$\mathbf{x}_k = \begin{bmatrix} x_{1,k+1} \\ x_{2,k+1} \\ x_{3,k+1} \\ x_{4,k+1} \end{bmatrix} = \begin{bmatrix} x_{1,k} \\ x_{2,k} \cdot x_{1,k} \\ x_{3,k} \\ x_{4,k} \cdot x_{3,k} \end{bmatrix} \tag{6}$$

which is a set of first order difference equations (or a recursive relationship) that can be expressed as

$$\mathbf{x}_{k+1} = \mathbf{f}(\mathbf{x}_k) \tag{7}$$

Note that the power system sampled signal in (3) can be obtained from the states in (6) as

$$z_k = \begin{bmatrix} 0 & \frac{1}{2} & 0 & \frac{1}{2} \end{bmatrix} \mathbf{x}_k \tag{8}$$

B. The Extended Kalman Filter

The EKF estimates the states of a nonlinear system of the form

$$\mathbf{x}_{k+1} = \mathbf{f}(\mathbf{x}_k) + \mathbf{w}_k \tag{9}$$

where $\mathbf{x}_k \in \mathbb{R}^n$ is the system (process) state vector at the kth step, $\mathbf{f}(\ldots)$ is the vector of functions that define the system's dynamics, and $\mathbf{w}_k \in \mathbb{R}^n$ is the vector with the process noise at step k. The measurement of the nonlinear system is assumed to be of the form

$$\mathbf{z}_k = \mathbf{h}(\mathbf{x}_k) + \nu_k \tag{10}$$

where $\mathbf{z_k} \in \mathbb{R}^m$ is the vector with the measurement (observation) at the kth step, $\mathbf{h}(\ldots)$ is the vector of measurement functions, and $\nu_k \in \mathbb{R}^m$ is the vector with the measurement noise at step k. The statistics of $\mathbf{w}_k$ and ν_k are assumed to be known and defined by

$$E[w_k] = 0 \quad E[w_k w_k^\top] = \mathbf{Q}_k \quad E[w_k w_j^\top] = 0 \text{ for } k \neq j \tag{11}$$

$$E[v_k] = 0 \quad E[v_k v_k^\top] = \mathbf{R}_k \quad E[v_k v_j^\top] = 0 \text{ for } k \neq j \tag{12}$$

$$E[w_k v_j^\top] = 0 \text{ for all } k \text{ for all } j \tag{13}$$

Additionally, it is assumed that the process and measurement noise covariances are independent of time, i.e. $\mathbf{Q}_k = \mathbf{Q}$ and $\mathbf{R}_k = \mathbf{R}\ \forall\ k$. The EKF algorithm, which is an adapted version of the classical KF algorithm for linear systems, is presented as follows.

Algorithm 1: Extended Kalman Filter

Time Update (or Predictor Update)

1 Predict the state:

$$\hat{\mathbf{x}}_k^- = \mathbf{f}(\hat{\mathbf{x}}_{k-1})$$

2 Linearize the system:

$$\mathbf{F}_{k-1} = \left.\frac{\partial \mathbf{f}(\mathbf{x})}{\partial \mathbf{x}}\right|_{\mathbf{x}=\hat{\mathbf{x}}_{k-1}}$$

3 Predict the covariance:

$$\mathbf{P}_k^- = \mathbf{F}_{k-1}\mathbf{P}_{k-1}\mathbf{F}_{k-1}^\top + \mathbf{Q}$$

Measurement update (or filter update)

4 Linearize the measurement:

$$\mathbf{H}_k = \left.\frac{\partial \mathbf{h}_k(\mathbf{x})}{\partial \mathbf{x}}\right|_{\mathbf{x}=\hat{\mathbf{x}}_k^-}$$

5 Measurement residual:

$$\mathbf{e}_k = \mathbf{z}_k - \mathbf{h}(\hat{\mathbf{x}}_k^-)$$

6 Measurement covariance:

$$\mathbf{S}_k = \mathbf{H}_k\mathbf{P}_k^-\mathbf{H}_k^\top + \mathbf{R}$$

7 Compute the Kalman Gain:

$$\mathbf{K}_k = \mathbf{P}_k^- \mathbf{H}_k^\top \mathbf{S}_k^{-1}$$

8 Update the state:

$$\hat{\mathbf{x}}_k = \hat{\mathbf{x}}_k^- + \mathbf{K}_k \mathbf{e}_k$$

9 Update the covariance:

$$\mathbf{P}_k = (\mathbf{I} - \mathbf{K}_k \mathbf{H}_k)\mathbf{P}_k^-$$

For the system model described in Subsection II-A, there are four states hence $n = 4$, the observation is a scalar and $m = 1$. Additionally, the linearization of (7) and (8) gives

$$\mathbf{F}_k = \left.\frac{\partial \mathbf{f}(\mathbf{x})}{\partial \mathbf{x}}\right|_{\mathbf{x}=\hat{\mathbf{x}}_k} = \begin{bmatrix} 1 & 0 & 0 & 0 \\ x_{2,k} & x_{1,k} & 0 & 0 \\ 0 & 0 & 1 & 0 \\ 0 & 0 & x_{4,k} & x_{3,k} \end{bmatrix} \tag{14}$$

$$\mathbf{H}_k = \left.\frac{\partial \mathbf{h}_k(\mathbf{x})}{\partial \mathbf{x}}\right|_{\mathbf{x}=\hat{\mathbf{x}}_k^-} = \begin{bmatrix} 0 & \frac{1}{2} & 0 & \frac{1}{2} \end{bmatrix} \tag{15}$$

C. The Unscented Kalman Filter

1) The Unscented Transform: The unscented transform is a method of estimating the statistics of a random variable after a nonlinear transformation is applied to it [10]–[12]. Let $\mathbf{x} \in \mathbb{R}^L$ be a vector of random variables that undergoes a nonlinear transformation $\mathbf{f}$ (i.e. $\mathbf{y} = \mathbf{f}(\mathbf{x})$). Let $\bar{\mathbf{x}}$ and $\mathbf{P}_\mathbf{x}$ be, respectively, the mean and a the covariance matrix of $\mathbf{x}$ then the unscented transform to compute the statistics of $\mathbf{y}$ is as follows

$$\boldsymbol{\mathcal{X}}_0 = \bar{\mathbf{x}} \tag{16}$$

$$\boldsymbol{\mathcal{X}}_i = \bar{\mathbf{x}} + \sqrt{(L+\lambda)\mathbf{P}_\mathbf{x}} \qquad i = 1, \ldots, L \tag{17}$$

$$\boldsymbol{\mathcal{X}}_i = \bar{\mathbf{x}} - \sqrt{(L+\lambda)\mathbf{P}_\mathbf{x}} \qquad i = L+1, \ldots, 2L \tag{18}$$

with

$$\lambda = \alpha^2(L+\kappa) - L \tag{19}$$

Propagating $\boldsymbol{\mathcal{X}}_i$ through the nonlinear function $\mathbf{f}$ yields

$$\boldsymbol{\mathcal{Y}}_i = \mathbf{f}(\boldsymbol{\mathcal{X}}_i) \qquad i = 0, \ldots, 2L \tag{20}$$

then the mean and covariance of the output points are determined by

$$\bar{\mathbf{y}} \approx \sum_{i=0}^{2L} W_i^{(m)} \boldsymbol{\mathcal{Y}}_i \tag{21}$$

$$\mathbf{P}_\mathbf{y} \approx \sum_{i=0}^{2L} W_i^{(c)} \{\boldsymbol{\mathcal{Y}}_i - \bar{\mathbf{y}}\}\{\boldsymbol{\mathcal{Y}}_i - \bar{\mathbf{y}}\}^\top \tag{22}$$

with the weights determined by

$$W_0^{(m)} = \frac{\lambda}{L+\lambda} \tag{23}$$

$$W_0^{(c)} = \frac{\lambda}{L+\lambda} + (1 - \alpha^2 + \beta) \tag{24}$$

$$W_i^{(m)} = W_i^{(c)} = \frac{1}{2(L+\lambda)} \qquad i = 1, \ldots, 2L \tag{25}$$

2) The Unscented Kalman Filter (with additive noise): The UKF addresses the same problem as the EKF. The system and measurement are again defined, respectively, by equations (9), and (10). The main difference with the EKF is that the UKF uses the unscented transform in the time update and measurement update stages to more accurately predict and update the state and covariance of the process, respectively. The UKF algorithm is presented as follows.

Algorithm 2: Unscented Kalman Filter

Time Update (or Predictor Update)

1 Compute the sigma points:

$$\boldsymbol{\mathcal{X}}_{k-1} = \Big[\hat{\mathbf{x}}_{k-1},\ \hat{\mathbf{x}}_{k-1} + \sqrt{(L+\lambda)\mathbf{P}_{k-1}},\ \hat{\mathbf{x}}_{k-1} - \sqrt{(L+\lambda)\mathbf{P}_{k-1}}\Big]$$

2 Propagate the sigma points through the process:

$$\boldsymbol{\mathcal{X}}_k^- = \mathbf{f}(\boldsymbol{\mathcal{X}}_{k-1})$$

3 Predict the state:

$$\hat{\mathbf{x}}_k^- = \sum_{i=0}^{2L} W_i^{(m)} \boldsymbol{\mathcal{X}}_{i,k}^-$$

4 Predict the covariance:

$$\mathbf{P}_k^- = \sum_{i=0}^{2L} W_i^{(c)} \left[\boldsymbol{\mathcal{X}}_{i,k}^- - \hat{\mathbf{x}}_k^-\right]\left[\boldsymbol{\mathcal{X}}_{i,k}^- - \hat{\mathbf{x}}_k^-\right]^\top + \mathbf{Q}$$

Measurement update (or filter update)

5 Propagate the sigma points through the measurement:

$$\boldsymbol{\mathcal{Z}}_k^- = \mathbf{h}(\boldsymbol{\mathcal{X}}_{k-1})$$

6 Update the measurement:

$$\hat{\mathbf{z}}_k^- = \sum_{i=0}^{2L} W_i^{(m)} \boldsymbol{\mathcal{Z}}_{i,k}^-$$

7 Measurement residual:

$$\mathbf{e}_k = \mathbf{z}_k - \hat{\mathbf{z}}_k^-$$

8 Compute measurement covariance and cross-covariance:

$$\mathbf{P}_{\mathbf{z}_k\mathbf{z}_k} = \sum_{i=0}^{2L} W_i^{(c)} \left[\mathcal{Z}_{i,k}^- - \hat{\mathbf{z}}_k^-\right]\left[\mathcal{Z}_{i,k}^- - \hat{\mathbf{z}}_k^-\right]^\top + \mathbf{R}$$

$$\mathbf{P}_{\mathbf{x}_k\mathbf{z}_k} = \sum_{i=0}^{2L} W_i^{(c)} \left[\mathcal{X}_{i,k}^- - \hat{\mathbf{x}}_k^-\right]\left[\mathcal{Z}_{i,k}^- - \hat{\mathbf{z}}_k^-\right]^\top$$

9 Compute the Kalman Gain:

$$\mathbf{K}_k = \mathbf{P}_{\mathbf{x}_k\mathbf{z}_k}\mathbf{P}_{\mathbf{z}_k\mathbf{z}_k}^{-1}$$

10 Update the state:

$$\hat{\mathbf{x}}_k = \hat{\mathbf{x}}_k^- + \mathbf{K}_k\mathbf{e}_k$$

11 Update the covariance:

$$\mathbf{P}_k = \mathbf{P}_k^- - \mathbf{K}_k\mathbf{P}_{\mathbf{z}_k\mathbf{z}_k}\mathbf{K}_k^\top$$

III. Frequency and RoCoF Estimation and Correction of Estimates

A. Frequency and RoCoF Estimation

Estimating frequency from point on wave data using any either the EKF and UKF approaches is done by realizing that states $x_{1,k}$ and $x_{3,k}$ have information related to the underlying frequency of the observation. The estimated frequency at the t_k instant, denoted $\hat{f}_k$, can be obtained by[1]

$$\hat{f}_k = \frac{f_s}{2\pi}\cos^{-1}\left(\frac{x_{1,k}+x_{3,k}}{2}\right) \tag{26}$$

where f_s is the sampling frequency (the inverse of T_s). To estimate the RoCoF this paper uses the simplest approach which is a finite difference between two adjacent points

$$\widehat{\mathrm{RoCoF}}_k = \frac{\hat{f}_k - \hat{f}_{k-1}}{T_s} \tag{27}$$

B. Correction of Estimates

The estimation of frequency by relationship (26) produces excellent results when the observed signal has the form in (2). However, power system signals following a disturbance do not follow the representation in (2). These signals are usually heavily distorted and, for brief periods of time, may no longer be sinusoidal waveforms. Estimating frequency under this circumstances is a challenge and most of the approaches yield inaccurate results. The main reason for this is that frequency itself may be *ill-defined* for a distorted signal. This work proposes using the *residual* of the EKF, step 5 in Algorithm 1 (step 7 in Algorithm 2 for the UKF case), as a signal to determine when $\hat{f}_k$ is inaccurate. In cases where $\hat{f}_k$ is deemed incorrect the output frequency will be hold to the previous non-faulty value. The algorithm for frequency correction is presented in Algorithm 3. In this algorithm, ϵ is a threshold value, $\hat{f}_{\mathrm{avg}}$ is the average of frequency estimates before t_k, and t_{hold} is the minimum time a frequency is held after the threshold value has been last surpassed. The algorithm uses a variable, $t_{\mathrm{cont,k}}$, to determine when the frequency estimate should no longer be corrected. This variable is initialized at zero. Note that this algorithm is performed at each time step t_k, is only enabled after the EKF or UKF estimator has settled and the initial value of HoldFlag is False.

[1]An alternative approach to compute the frequency is: $f_k = \frac{f_s}{2\pi}\left|\mathrm{Im}\left[\log(x_{1,k})\right]\right|$

Algorithm 3: Frequency Correction Algorithm

```
if e_k < ε and HoldFlag is False then
    f̂_k^corr = f̂_k
else if e_k < ε and HoldFlag is True then
    if t_cont,k < t_hold then
        HoldFlag ← False
    end
    f̂_k^corr = f̂_avg
    t_cont,k = t_cont,k−1 + T_s
else if e_k > ε then
    f̂_k^corr = f̂_avg
    Reset time: t_cont,k = 0
    HoldFlag ← True
end
```

IV. Results for POW Data with Phase Jumps

A. Synthetic POW Data

This section presents the results of estimating frequency of point on wave data with phase jumps. These data, referred to as synthetic data, was developed as follows

$$s(t) = A\cos(\omega t + \phi_H(t)) \tag{28}$$

where $\phi_H(t)$ is a Heaviside step defined as

$$\phi_H(t) = \begin{cases} \phi_{\mathrm{step}}, & \text{if } t > t_{\mathrm{step}} \\ 0, & \text{otherwise} \end{cases} \tag{29}$$

and t_{step} was varied such that the phase steps occurred at different instants of the sinusoidal waveform and around the same starting time of 2 seconds. The phase steps considered were of -0.3 rad (i.e. $\phi_{\mathrm{step}} = -0.3$) and this value was selected because it is the strongest recommended value for this type of signal in ref. [1]. The sampling rate of this data is set to 4.8 kHz ($T_s = 208.33\mu s$). The values selected for the correction algorithm are $\epsilon = 0.018$, and $t_{\mathrm{hold}} = 50$ ms (3 cycles).

Fig. 1a shows the synthesized POW data for the case where the phase jumps occur right when the sinusoidal waveform passes through the origin (or near 0°). On a different time scale Figs. 1b, 1c, and 1d respectively show the residual, the estimated frequency with its correction and the estimated RoCoF with its correction for both the EKF and UKF methods analyzed in this work. The residuals for both the EKF and UKF in Fig. 1b spike immediately after the phase jumps occurs and they both reach relatively *high* values for about 30 ms after the event. Fig. 1c shows the estimated frequency

by both the EKF and UKF methods as well as the corrected values. These results show that the considered phase jump is interpreted by the frequency estimators as a big drop in the frequency estimate. The corrected frequency estimates show that the proposed algorithm is able to *fix* the estimates and completely avoid the large frequency drops. Fig. 1d shows the estimated and corrected RoCOF. These results are obtained from the signals in Fig. 1c using the relationship in (27). Note that the corrected results of frequency and ROCOF would be preferred for any control application that uses either the frequency such as load shedding, or RoCoF such as synthetic or virtual inertia.

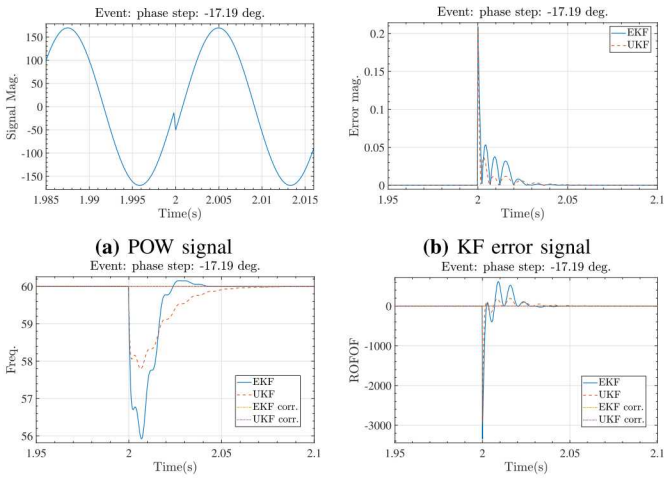

(a) POW signal **(b)** KF error signal

(c) Estimated frequency by the KF algorithms **(d)** Estimated ROCOF by the KF algorithms

Fig. 1: Frequency estimation when the step in phase, of -0.3 rad, occurs when the sinusoidal waveform is passing through the origin in an upward trend (equivalent angle of 0°).

Figs. 2 and 3 show respectively the same results as Fig. 1 for the cases where the waveform goes in an upward trend. Figs. 2 shows the case when the step in phase occurs for when the waveform is reaching about 70% of its amplitude (roughly 45°), and Fig. 3 the case when waveform is about to reach its maximum (roughly 90°). The results show that a phase jump occurring near the peak of the sinusoid yield a larger frequency drop in the uncorrected estimate. The results also show that the proposed corrector is able to identify and remove these large jumps in estimated frequency.

B. Simulated POW Data

This section presents the results of frequency estimation and correction for waveforms exhibiting phase jump-like distortions. The data presented here was obtained using the Simscape toolbox from MATLAB/Simulink.

Fig. 4a shows a distorted waveform that is the product of a line-to-line fault occurring at an adjacent bus in a power system. The fault occurred at 5 seconds, had a duration of 10 ms, and was between phases A and B. The signal to analyze corresponds to phase B and was selected because of the distortion it exhibited. Fig. 4b shows the residual e_k for the EKF and UKF approaches for the signal in Fig. 4a. The

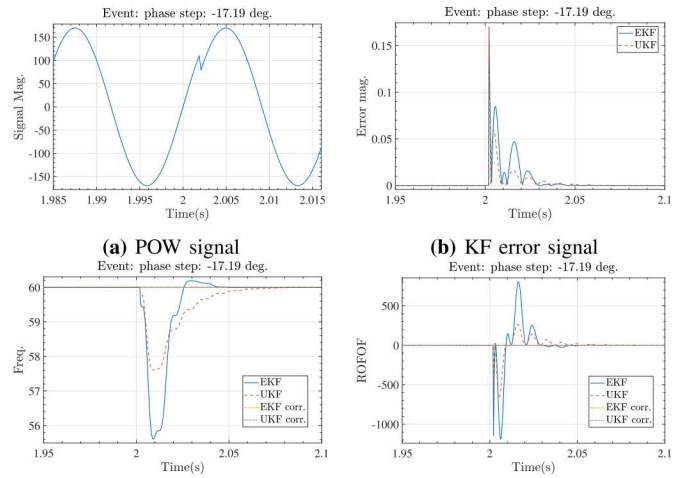

(a) POW signal **(b)** KF error signal

(c) Estimated frequency by the KF algorithms **(d)** Estimated ROCOF by the KF algorithms

Fig. 2: Frequency estimation when the step in phase, of -0.3 rad, occurs when the sinusoidal waveform is reaching about 70% of its amplitude in an upward trend (equivalent angle of 45°).

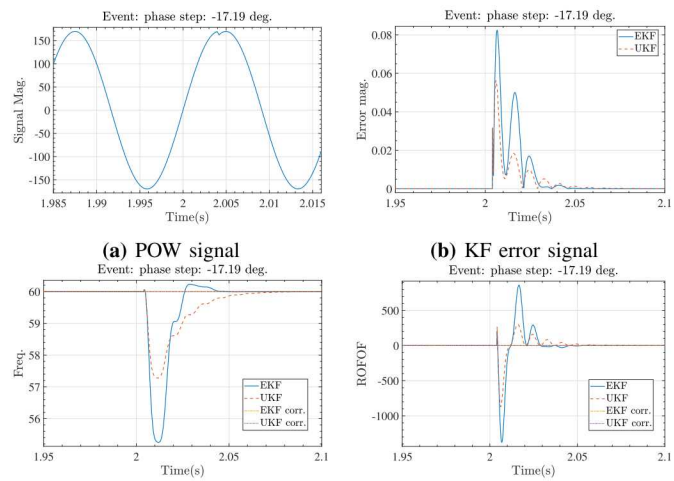

(a) POW signal **(b)** KF error signal

(c) Estimated frequency by the KF algorithms **(d)** Estimated ROCOF by the KF algorithms

Fig. 3: Frequency estimation when the step in phase, of -0.3 rad, occurs when the sinusoidal waveform is reaching its maximum in an upward trend (equivalent angle of 90°).

residual of both frequency estimation approaches increases right when the fault occurs and its value continues to be elevated for about 40 ms after the fault is cleared. Figs. 4c and 4d show, respectively, the initial and corrected frequency and RoCoF for both KF methods. These results show that the distortions in the sinusoidal waveform in Fig. 4a caused by the occurrence of the fault and its clearance are estimated as a steep increase followed by a considerable decrease in frequency. The corrected estimates using Algorithm 3 show that it is able to completely ride through this event and produce a steady frequency estimate. Note that for a control application that uses either the frequency or the RoCoF as a signal the corrected estimate is preferable; it is better to not act than to act improperly.

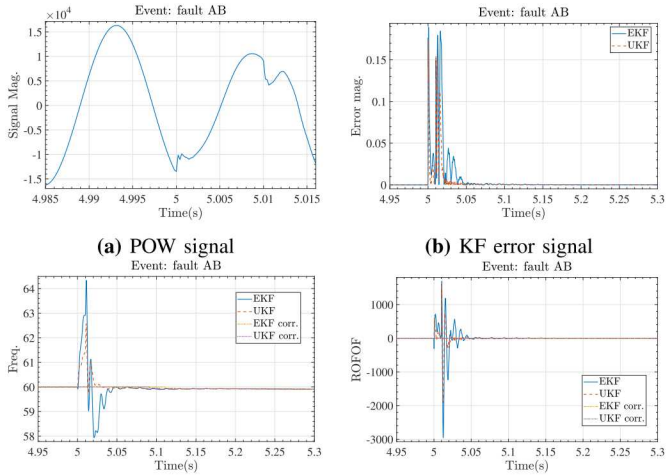

(a) POW signal **(b)** KF error signal

(c) Estimated frequency by the KF algorithms **(d)** Estimated ROCOF by the KF algorithms

Fig. 4: Frequency estimation for a waveform obtained from a line to line fault with duration of 10ms.

Fig. 5a shows a distorted waveform obtained from a line-to-line fault between phases A and B at a nearby bus. The fault was cleared after 50 ms and the waveform in the figure corresponds to phase C. Figs. 5b, 5c, and 5d respectively show the residual, the estimated frequency with its correction and the estimated RoCoF with its correction for both of the KF-based methods analyzed in this research. The results of these figures follow the same trend as those presented previously: (i) for both the EKF and UKF methods the residual spikes when the disturbance occurs, (ii) the frequency estimate for the distortion is reflected in a higher value followed by a drop, and (iii) the correction algorithm proposed is able to successfully correct the frequency estimate for both KF approaches.

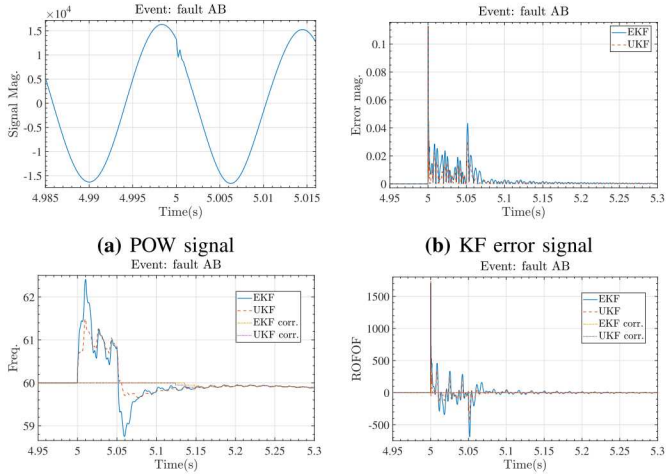

(a) POW signal **(b)** KF error signal

(c) Estimated frequency by the KF algorithms **(d)** Estimated ROCOF by the KF algorithms

Fig. 5: Frequency estimation for a waveform obtained from a line to line fault with duration of 50ms.

V. Conclusions and Future Work

This paper assesses the impact of phase steps on Kalman Filter frequency estimation algorithms. Both the EKF and UKF were considered. The paper shows that sudden phase jumps can be *falsely* identified as large frequency fluctuations. Based on the residual of the KF methods, the paper proposes a correction technique to identify when the frequency estimate is incorrect. For incorrect estimates the paper proposes a solution by holding the estimate to a previous value that was deemed correct. The performance of the proposed correction algorithm was demonstrated using both synthetic and simulated distorted waveforms.

A continuation of this work will include analyzing the frequency estimation techniques used here and the proposed correction algorithm with different data from other type of events such as load connection and faults to ground. Future work will also include studying how the frequency corrector can be improved by using an adaptive threshold.

References

[1] G. Rietveld, D. Colangelo, A. J. Roscoe, J. Kevin, and P. Wright, "Evaluation report on the problem of rocof measurement in the context of actual use cases and the "wish list" of accuracy and latency from an end-user point of view." EURAMET, Tech. Rep. 15NRM04 ROCOF, 2019.

[2] A. T. Phan, G. Hermann, and P. Wira, "Online frequency estimation in power systems: A comparative study of adaptive methods," in *Industrial Electronics Society, IECON 2014-40th Annual Conference of the IEEE*. IEEE, 2014, pp. 4352–4357.

[3] P. S. Wright, P. N. Davis, K. Johnstone, G. Rietveld, and A. J. Roscoe, "Field measurement of frequency and rocof in the presence of phase steps," *IEEE Transactions on Instrumentation and Measurement*, 2018.

[4] "1,200 MW fault induced solar photovoltaic resource interruption disturbance report – Southern California 8/16/2016," North American Electric Reliability Corporation (NERC), Altanta, GA, Tech. Rep. Version 1.1, June 2017.

[5] A. J. Roscoe, A. Dyśko, B. Marshall, M. Lee, H. Kirkham, and G. Rietveld, "The case for redefinition of frequency and rocof to account for ac power system phase steps," in *2017 IEEE International Workshop on Applied Measurements for Power Systems (AMPS)*. IEEE, 2017, pp. 1–6.

[6] A. Riepnieks, H. Kirkham, A. Faris, and M. Engels, "Phase jumps in pmu signal generators," in *2017 IEEE Power & Energy Society General Meeting*. IEEE, 2017, pp. 1–5.

[7] P. Dash, A. Pradhan, and G. Panda, "Frequency estimation of distorted power system signals using extended complex kalman filter," *IEEE Transactions on Power Delivery*, vol. 14, no. 3, pp. 761–766, 1999.

[8] H. Novanda, P. Regulski, F. M. González-Longatt, and V. Terzija, "Unscented kalman filter for frequency and amplitude estimation," in *PowerTech, 2011 IEEE Trondheim*. IEEE, 2011, pp. 1–6.

[9] P. K. Dash, G. Panda, A. Pradhan, A. Routray, and B. Duttagupta, "An extended complex kalman filter for frequency measurement of distorted signals," in *Power Engineering Society Winter Meeting, 2000. IEEE*, vol. 3. IEEE, 2000, pp. 1569–1574.

[10] E. A. Wan and R. Van Der Merwe, "The unscented kalman filter for nonlinear estimation," in *Proceedings of the IEEE 2000 Adaptive Systems for Signal Processing, Communications, and Control Symposium (Cat. No. 00EX373)*. Ieee, 2000, pp. 153–158.

[11] S. J. Julier and J. K. Uhlmann, "New extension of the kalman filter to nonlinear systems," in *Signal processing, sensor fusion, and target recognition VI*, vol. 3068. International Society for Optics and Photonics, 1997, pp. 182–194.

[12] S. J. Julier, "The scaled unscented transformation," in *Proceedings of the 2002 American Control Conference (IEEE Cat. No. CH37301)*, vol. 6. IEEE, 2002, pp. 4555–4559.